Characterization of Epoxies Cured with Bimodal Blends of Polyetheramines

Ian M. McAninch,[1,2] Giuseppe R. Palmese,[2] Joseph L. Lenhart,[3] John J. La Scala[1]

[1]Army Research Laboratory, ATTN: RDRL-WMM-C, Aberdeen Proving Ground, Maryland, 21005
[2]Department of Chemical and Biological Engineering, Drexel University, 3141 Chestnut Street, Philadelphia, Philadelphia, 19104
[3]Army Research Laboratory, ATTN: RDRL-WMM-G, Aberdeen Proving Ground, Maryland, 21005
Correspondence to: J. J. La Scala (E-mail: john.j.lascala.civ@mail.mil)

ABSTRACT: DGEBA was cured with bimodal blends of polyetheramines as well as with single molecular weight amines while maintaining stoichiometry. Glass transition temperatures (T_gs) and moduli were measured using dynamic mechanical analysis (DMA). Fracture properties were measured using the compact tension geometry and testing was performed at both ambient and non-ambient temperatures, investigating toughness changes as a function of temperature. For constant amine average molecular weights, the addition of high molecular weight amines caused increased glassy moduli at a constant $T - T_g$ and decreased densities while broadening the glass transition without changing the fracture toughness. The fracture behavior, specifically the slip-stick to brittle transition, was affected by the broadened transitions. T_g, breadth of T_g, and total damping were found to be proportional to the volume fraction of amine in the system. © 2013 Wiley Periodicals, Inc. J. Appl. Polym. Sci. 130: 1621–1631, 2013

INTRODUCTION

Epoxy resins are used in the composite industry because of their high modulus, glass transition temperature (T_g), and easy processability. The excellent properties arise from the highly cross-linked structure of the cured epoxy resins; however, their cross-linked structure leaves them with poor resistance to crack propagation. Extensive work has been done investigating the toughening of epoxy resins by incorporating additives such as rubber particles either preformed or formed *in situ*,[1,2] silica,[3,4] alumina,[5,6] glass beads, or polydimethylsiloxane.[7,8] Adjusting the epoxy to cure agent ratio and using mixtures of amines with different functionalities to control the cross-link density are other methods for improving epoxy toughness.[9–12] Also recent simulations have shown that the formation of microvoids in highly cross-linked systems can increase the toughness of the system through strain hardening.[13,14] The microvoids are formed by rearrangement of the molecules, with no bonds being broken. Recently, the toughness in vinyl esters was improved by using a bimodal blend of vinyl esters instead of a single molecular weight distribution.[15] Bimodal blends of epoxies cured with a single amine have also led to increased toughness, though the different molecular weight epoxies led to phase separation.[16] Other work with bimodal epoxy blends resulted in no change in properties compared to monodisperse epoxies, though both

the epoxy and amine contained similar phenol-based structures.[17] Instead of simply controlling the cross-link density, here we cure DGEBA with bimodal blends of structurally different polyetheramines with no phase separation. These blends will be compared to those of resins made with a single amine distribution.

EXPERIMENTAL

Blend Formulation

Epon 825 (Hexion Specialty Chem.), Figure 1(A), is a high purity diglycidyl ether of bisphenol A (DGEBA), with an epoxide equivalent weight of 176 g/mol. The amines used are Jeffamine® diamines (Huntsman) which are polyetheramines with the structure as shown in Figure 1(B). Three Jeffamines were used: D230, D400, and D2000, where *n* is approximately 2.6, 6.1, and 33, respectively, and have approximate molecular weights of 240, 445, and 1980 g/mol.

Several bimodal blends were considered. The first matched the amine hydrogen equivalent weight (AHEW) of D400 using a mixture of D230 and D2000. Matching the AHEW matches the molar average weight of the amine. Similar blends were made using D230/D2000 and D400/D2000 to match a theoretical amine with molecular weight of 1000 g/mol. Table I summarizes the blends and typical proportions of each component. The
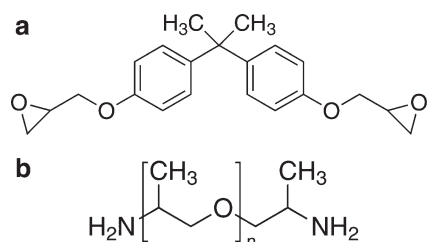
Figure 1. Structure of (A) Epon 825 (DGEBA) and (B) Jeffamine polyetheramines, n is ~2.8, 6.4, and 33 for D230, D400, and D2000, respectively.

AHEW for the Jeffamines were obtained from the manufacturer's certificates of analysis and slight batch-to-batch variations were observed and accounted for in the formulations. The AHEW for D230 ranged from 59.1 to 61.0, D400's was 111.1, while D2000's was either 495 or 500. In all cases, a stoichiometric amount of epoxy and amine were used, with two epoxide groups per amine.

Resin Cure

The Epon 825 was warmed to 45–50°C and degassed under vacuum to melt any crystallized material and to remove any volatiles. The appropriate masses of the Jeffamines were then added to the epoxies and were thoroughly mixed using an ARE 250 Thinky centrifugal mixer. The mixed resins were then degassed under vacuum just long enough for any trapped air to foam and collapse, for generally fewer than 5 min. The resin was then poured into molds, silicone rubber or aluminum, and cured for 2 h at 80°C. The samples were then removed from the mold and post cured for two hours at 125°C. Mixtures of Epon 825 and Jeffamine D2000 reacted more slowly than other formulations and were not gelled after 2 h at 80°C; those samples were instead cured at 125°C for 4 h. All cured samples were transparent indicating that phase separation did not occur.

Extent of Cure

The extent of cure for all samples was tested in a TA Instruments Q1000 DSC. About 5–10 mg of freshly prepared sample was sealed in hermetic aluminum DSC pans and tested

according to the desired cure and post cure schedule described above. After the cure, the sample was quickly cooled to 0°C to quench the reaction, and then ramped at 5°C/min to 300°C to observe any residual cure. The total heat of cure was determined by taking 5–10 mg of uncured resins and ramping the temperature at 5°C/min from room temperature to 300°C. Under these conditions, the exothermic peak of the D2000 samples did not return to the baseline due to slower reaction; instead D2000 samples were ramped at 3°C/min to ensure there was a baseline for peak integration. The exothermic peak was integrated using TA Universal Analysis software; an average of at least three runs was used. For the full cure cycle samples, only the final ramp was examined for signs of an exothermic peak, signifying a residual heat of reaction.

Near-infrared (NIR) spectroscopy was also used to investigate the extent of cure. In the NIR region, epoxide groups show peaks at 4530 and 6060 cm^{-1}; primary amines have a peak at 4925 cm^{-1} while a peak at 6534 cm^{-1} is caused by primary and secondary amines.[18] Spectra of the neat monomers and the cured samples were taken using a Nicolet Nexus 870 infrared spectrometer. The spectra of the cured samples were qualitatively examined for residual epoxy or amine functionality.

Polymer Characterization

Samples with approximate dimensions of 35 × 12 × 3.25 mm were tested on a TA Instruments Q800 Dynamic Mechanical Analyzer using the single cantilever clamp, operating at 1 Hz with 7.5 μm displacement. Due to its low modulus above T_g, the 825/D2000 samples required thicker samples (5–5.5 mm) to yield valid results in the rubbery region; however, since altering the aspect ratio of samples can affect the modulus, only rubbery modulus data was used from the thicker samples.[19] The starting temperature depended on the glass transition temperature of the sample. After an appropriate equilibration period, longer for lower starting temperatures, the temperature was increased by 2°C/min to 160°C. To compare samples with a similar thermal history, samples of each resin were cooled to −100°C then allowed 60 minutes to reach equilibrium before increasing the temperature by 2°C/min to 160°C. The clamps were tightened after approximately 30 min at −100°C.

Table I. Amounts of Amine per 100 g Epon 825

	Mass of D230 (pph)	Mass of D400 (pph)	Mass of D2000 (pph)	Total Amine (pph)	MW amine (g/mol) (mol avg)
D230	34.3	0	0	34.3	240
D400	0	63.1	0	63.1	445
D2000	0	0	281.3	281.3	1980
B270 (D230)	33.8	0	4.6	38.4	270
B390 (D230)	31.4	0	24.3	55.7	390
B440 (D230)	30.3	0	32.8	63.1	440
B620 (D400)	0	56.0	31.7	87.7	620
B1000 (D230)	19.3	0	122.7	142.0	1000
B1000 (D400)	0	40.3	101.7	142.0	1000

A prefix of D# signifies a resin made using a single amine of weight # while B# signifies a bimodal blend with an average amine weight of #. The lower molecular weight component of the blend is indicated in parentheses.

Table II. Measured and Calculated Heats of Cure

Resin	ΔH_{cure} (measured) (J/g)	ΔH_{cure} (calculated) (J/g)
D230	521 ± 5	–
D400	458 ± 10	428
D2000	169 ± 8	183
B270 (D230)	500 ± 10	503
B390 (D230)	458 ± 15	449
B440 (D230)	429 ± 22	428
B620 (D400)	368 ± 19	372
B1000 (D230)	291 ± 7	288
B1000 (D400)	287 ± 2	288

The temperature at which the peak in the loss modulus occurred was considered the glass transition temperature of the resin.[20] All samples had a definite point in the loss modulus where the rubbery modulus began to increase with increasing temperature; this point was used to calculate the molecular weight between cross-links, M_c. The theory of rubber elasticity was used to calculate the cross-link density, v, eq. (1), or M_c, eq. (2), from dynamic mechanical analysis (DMA) data:

$$v = \frac{E'}{3RT} \qquad (1)$$

$$M_c = \frac{3RT\rho}{E'} \qquad (2)$$

Where R is the gas constant, T the absolute temperature, ρ the density, and E' the modulus of the rubbery plateau. Rubber elasticity applies to polymers with low cross-link densities and may not give completely accurate cross-link density measurements for highly cross-linked epoxies.[21] Nonetheless, numerous researchers have used it as a measure of cross-link density and it seems to show good trends for sample sets with similar chemistries.[11,22]

The densities of all samples were measured using the water displacement method outlined in ASTM Standard D792-00. Thermal expansion data in both the rubbery and glassy regions were measured using a TA Instruments Q400 Thermomechanical analyzer. The coefficients of thermal expansion, CTE or α, was calculated by eq. (3):

$$\alpha = \frac{1}{l_0}\frac{\Delta l}{\Delta T} \qquad (3)$$

Where l_0 is the original length, Δl the change in length, and ΔT the change in temperature.

Samples were made, following the cure procedures described above, in aluminum molds measuring 10 × 10 × 55 mm. The molds were not completely filled, yielding samples approximately 6 × 10 × 55 mm. From these bars, smaller samples with nominal dimensions of 6 × 6 × 10 mm were cut. Samples were tested in the unaltered 10 mm direction and three to five samples per formulation were tested. A constant force of 0.05 N was used for both the preload and the applied load. Samples were heated from room temperature to 125°C, cooled to −70°C, then heated to 150°C at 3°C/min. The initial heating cycle was to remove any residual stress. The CTE values from the final cycle, from −70 to 150°C were used to calculate the density as a function of temperature assuming isotropic behavior.

Fracture toughness was measured on samples having T_gs above 40°C using the compact tension geometry and according to ASTM standard D5045. Samples were cured in silicone rubber molds with nominal dimensions of 1.2 × 1.25 × 0.5 inches. A 0.40″ notch was cut into each sample with a diamond saw. The samples and single edged razors were placed in a freezer overnight (approximately −20°C) to ensure all samples were well within their glassy region when starter cracks were made. Samples and razor blades were removed from the freezer; the razor was inserted into the notch and tapped with a hammer, until a crack propagated into the sample 0.35″ long, leaving a ligament of approximately 0.5″ for the crack to propagate through during testing. These cracks were of the "instantly propagated" type, shown by Ma et al. to give minimum K_{1c} values.[23] Samples were tested at −20, 0, 23, or 40°C after being conditioned at those temperatures for at least 2 h. Seven samples per test condition were tested, unless noted otherwise, and the average of the measurements was reported.

RESULTS AND DISCUSSION

Extent of Cure Analysis

Calculated heats of reaction for all samples were determined based on the measured heat of reaction of D230; these were compared to those measured. Since D230 is the shortest amine, the D230 resin is expected to have the least amount of steric hindrance and the most complete reaction. The heat of reaction for D230, $\Delta H_{cure, D230}$, was used as a reference to calculate ΔH_{cure} for the other resins. Theoretical heats of reaction for each resin were calculated by multiplying the reference $\Delta H_{cure, D230}$ (521 J/g) by the ratio of the concentration of epoxy groups in each resin to the concentration of epoxy groups in the D230 resin, as shown in eq. (4). The measured and calculated ΔH_{cure} are listed in Table II, and were similar in all cases. Also, no residual exothermic peaks were visible in any samples, signifying near complete reaction/cure. Full reaction, per DSC results, has also been reported for DGEBA reacted with short aliphatic amines.[24,25]

$$\Delta H_{cure} = \Delta H_{cure,D230} \times \frac{\text{mol Epoxy/g resin}}{\text{mol Epoxy/g resin}_{D230}} \qquad (4)$$

NIR spectra of the uncured monomers clearly showed the peaks attributed to the amine and epoxy functional groups. These peaks were no longer visible in the spectra of the cured samples, confirming the DSC results of complete reaction. When full conversion of epoxy resins is not achieved, residual secondary amine functional groups are evident in NIR spectra; however,

Table III. Summary of Density and DMA Results

Resin	Density at 25°C (g/cm³)	Glassy Density (T_g − 30°C) (g/cm³)	Modulus at 30°C (MPa)	T_g (°C)	Peak of tan δ (°C)	Breadth of transition (°C)	T_β (°C)
D230	1.157 ± 0.001	1.146 ± 0.001	2360 ± 70	91.9 ± 2.8	97.9 ± 2.2	11.2 ± 0.8	− 59
D400	1.138 ± 0.002	1.138 ± 0.002[a]	2370 ± 110	53.8 ± 0.3	59.0 ± 0.4	10.2 ± 0.4	− 68
D2000	1.060 ± 0.010	1.126 ± 0.011	2.0 ± 0.1[b]	− 37.4 ± 0.7	− 24.1 ± 1.0	19.9 ± 1.8	− 85
B270 (D230)	1.153 ± 0.002	1.143 ± 0.002	2460 ± 30	85.3 ± 1.2	92.7 ± 1.1	12.9 ± 0.6	− 53
B390 (D230)	1.145 ± 0.001	1.141 ± 0.001	2080 ± 40	61.7 ± 1.5	75.5 ± 0.3	19.5 ± 0.5	− 63
B440 (D230)	1.140 ± 0.009	1.139 ± 0.009	1740 ± 100	55.6 ± 0.8	69.8 ± 0.4	21.5 ± 0.5	− 64
B620 (D400)	1.125 ± 0.000	1.137 ± 0.000[a]	640 ± 50	28.2 ± 1.2	41.8 ± 0.3	16.5 ± 0.5	− 71
B1000 (D230)	1.094 ± 0.001	N/A	9.4 ± 0.9	− 26.9 ± 0.9	16.2 ± 0.9	37.2 ± 0.4	− 76
B1000 (D400)	1.096 ± 0.001	N/A	6.9 ± 0.8	− 18.9 ± 1.2	13.6 ± 2.0	23.4 ± 1.0	− 73

[a] Only one sample available for CTE measurements.
[b] values from thick DMA samples.

this is more typical in higher T_g, aromatic-cured epoxy systems.[18]

Polymer Properties

Table III summarizes the DMA and density results for the resin blends, with the breadth of transition being reported as the full width at half maximum of the tan δ curve; the properties had narrow distributions and no batch-dependent variations were observed provided stoichiometry was maintained. The room temperature densities steadily decrease as the average amine molecular weight increases and as the T_g of the resins decreases. By assuming isotropic samples, the CTE data was used to calculate volumetric changes with temperature and hence create density–temperature curves from the measured density values. These curves are plotted in Figure 2, shifted to $T − T_g$, using
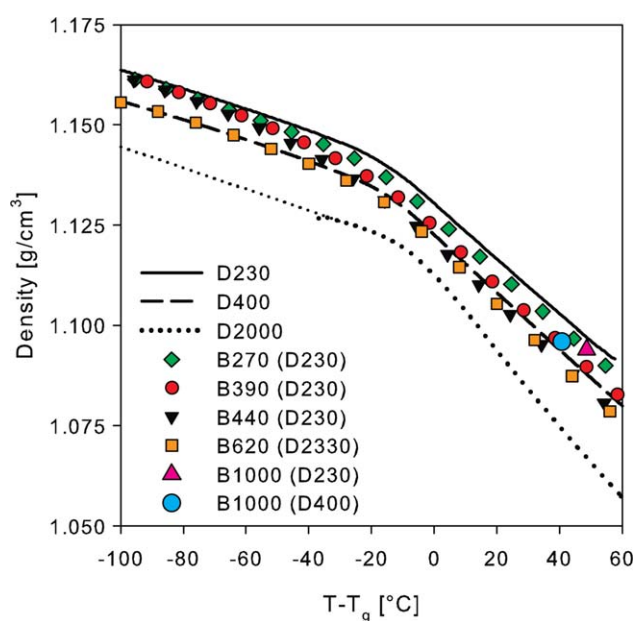
the peak of the loss curve as the T_g. The inflection in CTE, and hence density, data is also a measure of the T_g but here the inflections in the curves do not match up with 0 as different thermal lags exist between the CTE and DMA data due to the different sample dimensions and heating ramp rates. When shifted to $T − T_g$, it is observed that formulations containing any amount of D230 approach a density of 1.165 g/cm³ 100°C below their respective T_gs, while those containing D400 approach a lower density of 1.155 g/cm³. The sample containing only D2000 has the lowest density. While CTE data were not available for the B1000 blends, their measured room temperature densities are also plotted in Figure 2 and it appears they would follow the same trends as the other blends.

As mentioned previously, the temperature of the peak in the DMA loss modulus was used at the T_g. The loss modulus is plotted versus $T - T_g$ in Figure 3. The main or α relaxation is
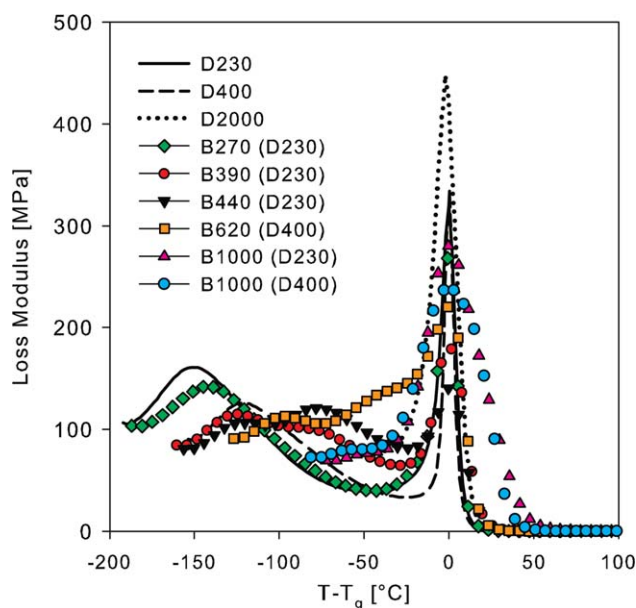

Figure 2. Density as a function of $T − T_g$ from CTE data. The dotted line for D2000 is a linear extrapolation to $T − T_g = − 100$ for comparison. [Color figure can be viewed in the online issue, which is available at wileyonlinelibrary.com.]

Figure 3. Loss moduli shifted to $T − T_g$. [Color figure can be viewed in the online issue, which is available at wileyonlinelibrary.com.]
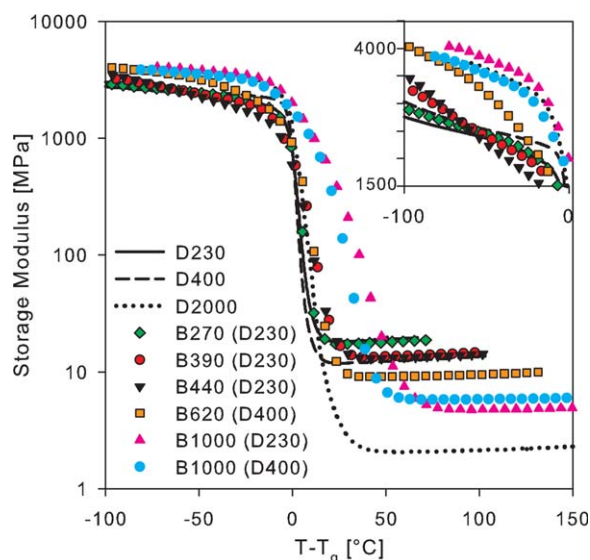
Figure 4. Storage moduli of representative samples versus $T - T_g$. Inset shows the glassy modulus on a linear scale. The D2000 data is a composite of a thin sample below T_g and a thick sample above to properly show rubbery modulus data. [Color figure can be viewed in the online issue, which is available at wileyonlinelibrary.com.]

the glass transition, T_g, whereas the secondary or β transition is also visible; both are listed in Table III. The beta relaxation (T_β) for epoxy resins is attributed to the relaxation of the hydroxy-propyl ether units [$-O-CH_2-CH(OH)-CH_2-$] and is known to occur between $-60°C$ and $-100°C$.[26,27] All T_β for these resins appear in that range. The epoxy T_β is known to shift to lower temperatures as the network changes from a highly cross-linked to a more linear polymer;[28] the same trend is observed here, with D2000 having the lowest T_β and D230 the highest. The magnitude of the beta peak in the loss modulus also decreases as the concentration of the hydroxypropyl ether groups decreases, with D230 having the strongest transition and B1000 (D230), B1000 (D400), and D2000 all having very weak transitions.

Comparing the resins with single amines, the D2000 exhibits the largest loss modulus, followed by D400 and D230, whereas the opposite is seen in the T_gs, with D2000 having the lowest. While the magnitude of the loss peak for the blends does not follow a trend, there is a trend of decreasing T_g with increasing average amine molecular weight. For some samples, especially B390 (D230), B440 (D230), and B620 (D400) a third peak or shoulder appears in the loss modulus around $-20°C$. This peak is near that of D2000 ($-37°C$) and suggests there is micro-phase separation with a D2000-rich phase, however since these samples are optically clear, the domains must be small.

Comparing the breadth of tan δ at half maximum, as listed in Table III, to the storage modulus curves in Figure 4, the breath of the tan δ at half maximum appears to be a reasonable measure of the breadth of the glass transition. D230, D400, and B270 (D230) all reached their rubbery region at about the same temperature, $\sim10°C$ above T_g and all had similar breaths of transitions. B390 (D230), B440 (D230), B620 (D400), and

D2000 all reached their rubbery regions about 20°C above T_g, which is reflected in full width at half maximum tan δ values of approximately 20°C. Both B1000 blends did not reach their rubbery regions until 25–40°C above T_g. All of the tan δ curves are shown in Figure 5, plotted against $T - T_g$. This figure also shows that in blends with higher D2000 content, the tan δ peak is shifted to higher temperatures relative to the T_g due to the increased broadness of the transition. Here it appears that certain blends of low and high molecular weight polyetheramines can greatly broaden the glass transition without changing its location.

To easily view modulus trends, the modulus data were plotted versus $T - T_g$, and are shown in Figure 4. With regards to the single amine resins, there was a trend of higher glassy modulus with increasing amine molecular weight at a given distance below T_g. This trend was seen elsewhere for epoxies cured with D230 and D400.[29] At a given offset below the T_g, as the amount of D2000 increased, the glassy modulus increased. At 75°C below T_g, the resins containing mostly D230 or D400 appeared to reach a plateau of 2500–3000 MPa while those containing more D2000 tracked towards or reached a plateau of 3500–4000 MPa. As mentioned earlier, the densities decreased with increasing D2000 content, so improved packing at lower temperatures does not explain the increased modulus. The increase in modulus with increasing amine molecular weight can be partially attributed to hydrogen bonding which can increase modulus values and is stronger at lower temperatures.[30] As the molecular weight of the amines increased, the number of hydroxyl groups and hence hydrogen bonds decreased; however, amine flexibility and the number of oxygens that can act as hydrogen acceptors also increased. Figure 6 shows the network structure of these resins, as n increases in the polyetheramines, the backbone oxygens have more flexibility to act as hydrogen
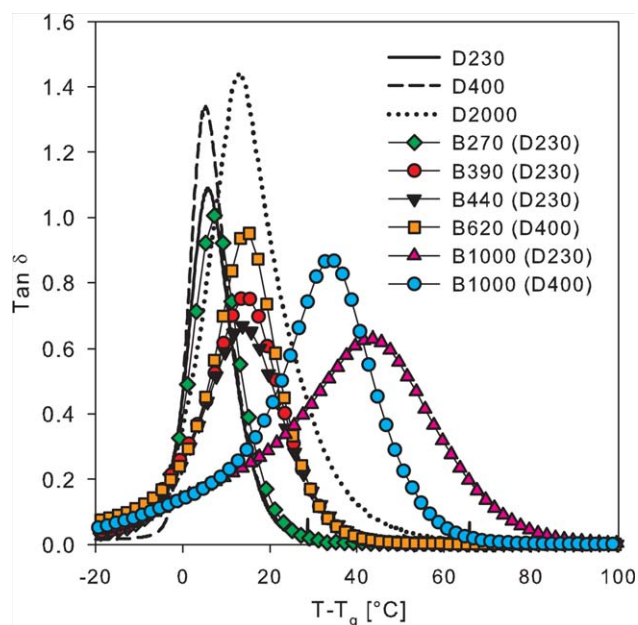

Figure 5. Tan δ curves for all resins, plotted versus $T - T_g$. [Color figure can be viewed in the online issue, which is available at wileyonlinelibrary.com.]
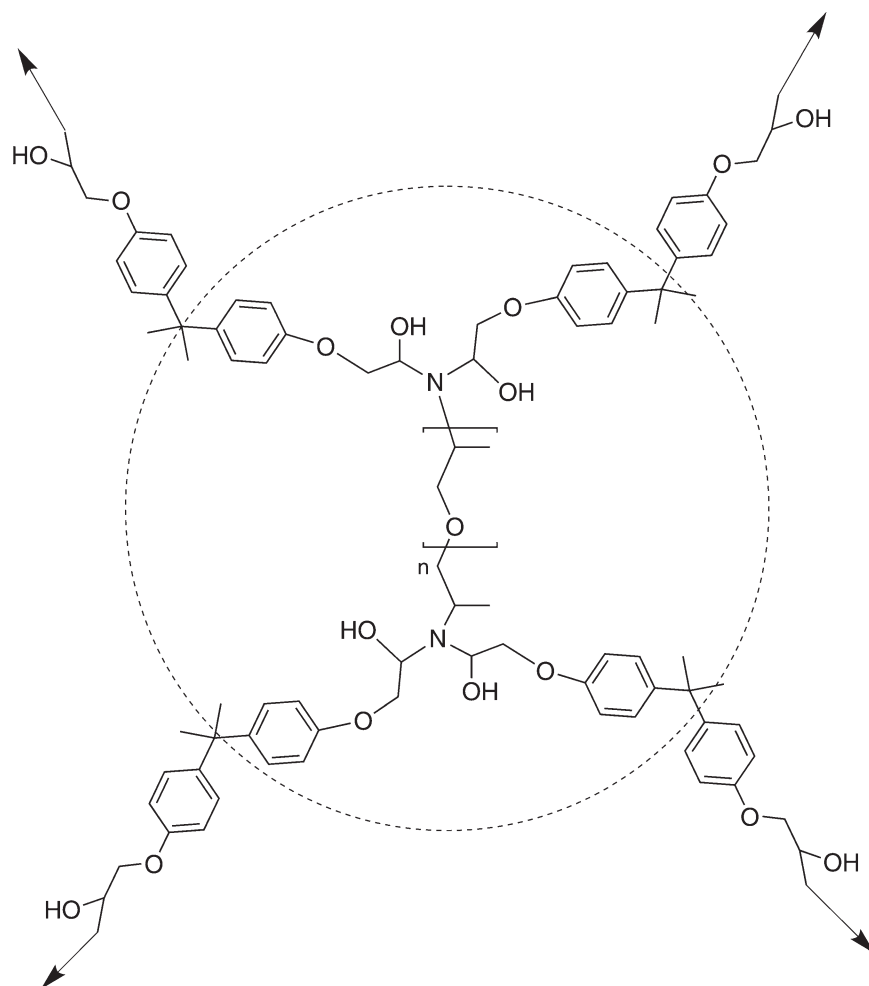
Figure 6. Ideal network structure: the circle encompasses one repeat unit, while the arrows extend into the network.

acceptors. Increased polyether flexibility is known to increase the extent of hydrogen bonding.[31] The modulus increase is also affected by the reduced T_gs. The resins with the highest moduli at 50°C below T_g, D2000, B1000 (D230), and B1000 (D400), also have the lowest T_gs. At 50°C below T_g for these resins is also below the beta relaxation of epoxies, -50 to -70°C, and the freezing of the hydroxypropyl ether units can increase the modulus.[26]

Three pairs of resins invite comparisons. The D230 and B270 (D230) resins had the highest and very similar T_gs, which was unsurprising given that the bimodal amine blend was over 85 wt % or 92 mol % D230. Interestingly, the storage modulus for the B270 (D230) blend is higher than that of D230 below 50–60°C ($T - T_g \sim -25$°C), but lower at higher temperatures (Figure 4). This modulus crossover cannot be explained by density variations, as the density for the D230 had the highest density at any temperature, as shown in Figure 2, nor T_β relaxations as this crossover is well above the T_β transitions. Instead the modulus crossover can be partially attributed to additional hydrogen bonding;[28,29] the B270 (D230) has approximately 20% more backbone oxygens than D230.

The B440 (D230) blend and D400 had the same AHEW and consequentially had the same T_g, though the blend had a broader glass transition. The storage modulus of the blend was approximately 1 GPa lower at 30°C ($T - T_g \sim -25$°C), but exceeded that of D400 at $T - T_g \sim -60$°C. The breadth of the transition for the B440 (D230) was twice as broad as that of the D400 alone, and similar to that of D2000. Above T_g, the density of B440 (D230) was lower than that of D400; however, below T_g, B440 (D230) had a higher density. This density crossover occurs at $T - T_g \sim -30$°C, approximately 30°C away from the modulus crossover. Despite the different crossover locations, the increased density at lower temperature can contribute to the higher modulus at lower temperature. In addition, different thermal lags due to the different sample dimensions and heating ramp rates in the thermomechanical analysis relative to DMA testing may also contribute to the crossover difference.

The two blends with AHEW values matching a hypothetical D1000 were less similar than expected. Their T_gs differed by approximately 10°C and the breadth of the transition was ~14°C broader for the blend using D230 rather than D400. The
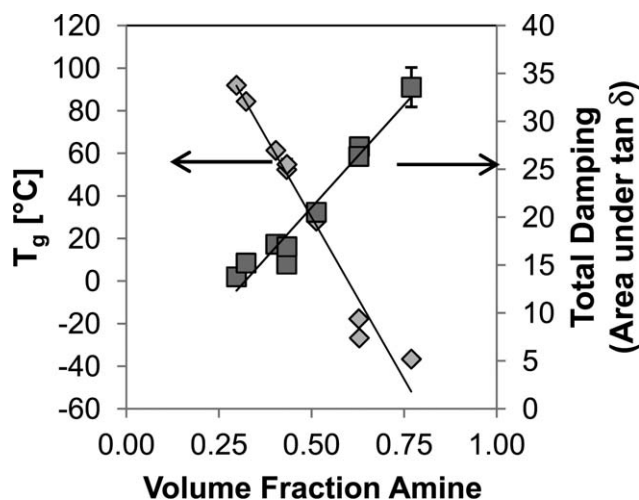
Figure 7. T_g and total damping versus volume fraction of amine.

B1000 (D230) resin contained more D2000 than any other bimodal blend and consequentially could have had more intramolecular cyclization during cure than the others.

The Fox equation predicts the T_g of a blend of polymers based on the individual glass transition temperature of the components i, T_{gi}, along with the weight fractions, w_i[32]:

$$\frac{1}{T_g} = \frac{w_a}{T_{ga}} + \frac{w_b}{T_{gb}} \qquad (5)$$

By treating the blends as mixtures of 825/D2000 with 825/D230 or 825/D400, the Fox equation gives reasonably good predictions, although it requires separate calculations for the D400 and the D230 blends, generating two curves. Instead, if T_g is plotted versus the volume fraction of amine, based upon uncured liquid volumes, a single linear trend is obtained, as shown in Figure 7. The largest deviation from the linear trend comes with the B1000 blends, which could be due to increased heterogeneity as the content of D2000 increased.

The breadth of the T_g increased with increasing amount of D2000 in the blends; however, it was not a simple function of
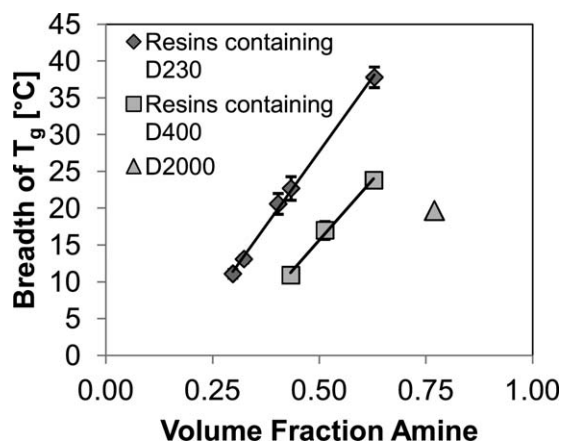
D2000 content. The broadening of the transition is often associated with heterogeneity in the network structure with different segments having low and high T_gs.[20] This is exhibited by the fact that B440 (D230) had a significantly broader glass transition than B620 (D400) while both had similar D2000 content. When plotted against the volume fraction of amine, it becomes clear that the breadth is dependent upon both the amine volume fraction as well as the type of amine, as shown in Figure 8.

In addition to broadening the tan δ, the blends also have decreased maximum dampening compared to the single amine resins. Even though the maximum damping is decreased, the total damping capacity increased with increasing amine molecular weight. The total damping was calculated by integrating the tan δ curves. Instead of specifying a temperature range to integrate, the integration limits were set at the temperatures where tan δ equaled 0.05 on either side of the tan δ peak. Increased damping means that the blends are more able to dissipate energy through viscous means than their single amine counterparts.[20] The total damping is also directly proportional to the amine volume fraction, as shown in Figure 7. The tan δ area is known to decrease with increasing cross-linking level and T_g for polyacrylates and it applies to these epoxy-amine networks as well.[33] The linear relationship and the similar damping of D400 and B440 (D230) suggests that, neglecting stoichiometry, a single D2000 molecule has similar damping compared to several molecules of D230 of equivalent molecular weight.

Cross-Link Density

There is a very strong trend of increased M_c with increased amine molecular weight. The experimental M_c values were calculated using eq. (2) and plotted in Figure 9 against the average amine molecular weight. The values for the moduli used in eq. (2) were taken from the minimum modulus value, whose location ranged from 26 to 82°C above T_g for the narrowest and broadest transitions, D400 and B1000 (D230), respectively. The temperature appropriate densities, as calculated by the CTE measurements were used except for the B1000 (D230) and
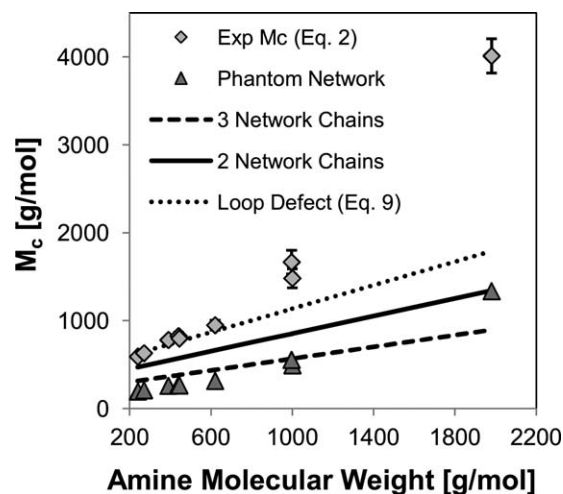

Figure 8. Breadth of T_g versus total amine volume fraction. The narrowest breaths of each line are from single amine resins.

Figure 9. Experimental and theoretical M_c values versus average amine molecular weight. The solid line represents eq. (7) and the dashed line eq. (8).

Table IV. Experimental M_c and Theoretical M_c Values Calculated Using eqs. (8) and (9)

Resin	M_c (experimental) (g/mol)	$M_{c(theo)}$ (eq. (8)) (g/mol)	$M_{c(single\ loop)}$ (eq. (9)) (g/mol)
D230	593 ± 25	315	629
B270 (D230)	632 ± 13	325	649
B390 (D230)	791 ± 14	365	729
B440 (D230)	826 ± 44	381	763
D400	798 ± 21	383	765
B620 (D400)	950 ± 54	441	883
B1000 (D400)	1553 ± 111	568	1136
B1000 (D230)	1762 ± 143	567	1133
D2000	4013 ± 195	895	1789

B1000 (D400) resins. Their densities were estimated to be 1.05 and 1.06 g/cm^3, respectively, based on their room temperature densities, the trends from the other formulations, and the distance above T_g at which those minima occurred. The M_c values are summarized in Table IV.

The D400 and B440 (D230) samples had nearly the same M_c, which was expected as the blend was designed to match D400. The M_c values of B1000 (D400) are also very similar, despite having T_gs almost 10°C apart.

Theoretical M_c values can be calculated in several ways. Scanlan calculated the molecular weight between cross-links using[34,35]:

$$M_c = \frac{W}{\sum_{f=3}^{\infty} \frac{f}{2} C_f} \tag{6}$$

where W is the weight of the network repeat unit, f is the functionality of the reactant, and C_f is the number of reactants f present in the repeat unit. This is simply the molecular mass of the repeat unit, divided by the number of network chains. Charlesworth stated that a short rigid diamine can effectively be considered a tetrafunctional point, $f = 4$ (two network chains), otherwise a diamine should be considered to be two tri-functional blocks, $f = 3$, ensuring that the backbone between the amine groups is considered as a network chain (three network chains).[36] In these two cases, M_c is given by eqs. (7) and (8), respectively, and the repeat unit can be depicted as shown in Figure 10:

$$M_c = \frac{Mw_{amine} + 4 \times \left(\frac{1}{2} \cdot Mw_{epoxy}\right)}{2} \tag{7}$$

or

$$M_c = \frac{\frac{1}{2} Mw_{amine} + 2 \times \left(\frac{1}{2} \cdot Mw_{epoxy}\right)}{\frac{3}{2}}$$
$$= \frac{Mw_{amine} + 4 \times \left(\frac{1}{2} \cdot Mw_{epoxy}\right)}{3} \tag{8}$$

The Jeffamines have backbone lengths varying from approximately 11 atoms for D230 to approximately 103 for D2000, so

given the flexible backbone, each amine molecule should be considered to be two tri-functional bodies and M_c should be governed by eq. (8). Additionally, these equations agree with the theory of Miller and Macosko,[37] whose theory reduces to Scanlan's in the limit of complete reaction, as was measured for these epoxy-amine resins systems.

Figure 9 also shows the results of eqs. (7) and (8). While the experimental data is closer to that of eq. (7), the larger amine molecules cannot be assumed to act as tetrafunctional points. Some work has measured M_c in epoxies to be similar to the theoretical value calculated by eq. (8). LeMay used DGBEA reacted with 4,4'-diaminodiphenyl sulfone (DDS) and measured slightly lower than expected M_cs,[38] possibly due to steric restrictions due to the bulky and rigid aromatic rings.[36] Nakka et al.[22] reacted a variety of short linear f functional amines with DGEBA and saw good agreement between theoretical values calculated in a method similar to eq. (7) and measured low values of M_c with amines containing 3–4 amine hydrogens, but the disagreement increased with increasing M_c as the number of amine hydrogens decreased. Crawford and Lesser[11] also had good agreement between theoretical and experimental values for stoichiometric blends of either linear or aromatic tri-functional amines and also for tetrafunctional amines but only for theoretical M_c values greater than 500–600 g/mol.

In this study, the agreement between theoretical and experimental M_cs is poorer and the difference increased with increasing amine molecular weight. In all the above-mentioned cases, the amines used were either aromatic or very short linear chains. Here, we have longer, flexible amines that are more mobile. Network mobility is often accounted for using the "phantom network" model, in which no physical interactions between adjacent chains are considered.[39,40] This model modifies the M_c calculation [eq. (2)] with a $\frac{f-2}{f}$ term, where f is the functionality of the cross-linking molecule, in this case . The results of applying this front factor to the experimental M_c calculations are also shown in Figure 9. The phantom network assumption reduces M_c below either of the two structural models for M_c. Since the assumption removes any physical interactions, it is often coupled with other terms that add back in the contributions of chain entanglements and non-Gaussian chain statistics.[36,38] Adding these contributions back will bring the M_c values in the range predicted by the structural model. More interesting is the fact that the experimental M_c values appear to follow two trends. Resins with amine blends 620 g/mol and below follow a slope that is similar to the model predictions, presumably because those networks have relatively few defects, while the
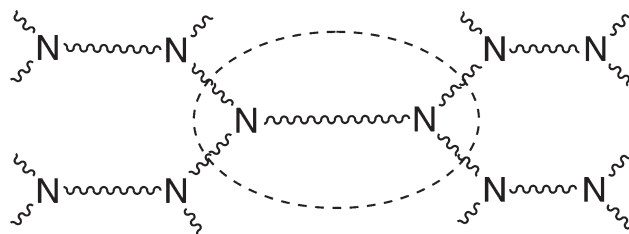

Figure 10. Sketch of the network structure. Wavy lines represent chains large enough to contribute to the network.
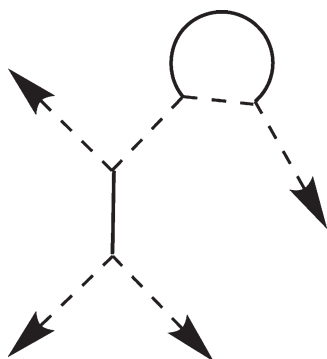
Figure 11. Sketch showing a single loop defect. Dashed lines represent epoxies, while solid represent amines; arrows extend out into the bulk network.

slope of those formulations with amine blends greater than 620 g/mol is much steeper. This deviation can be explained by cyclization. As the amount of D2000 increases in a resin, the potential for cyclization increases as the large molecule can bend around and react with the same epoxy or possibly creating small self contained areas in the network. These defects can substantially increase M_c; a simple single loop defect of D2000, as shown in Figure 11, would increase M_c by approximately 900 g/mol. If a single loop defect is considered, then eq. (8) becomes:

$$M_c = \frac{2 * Mw_{amine} + 4 \times \left(\frac{1}{2} \cdot Mw_{epoxy}\right) + 2 * Mw_{epoxy}}{3} \quad (9)$$

And the results, shown in Table IV and Figure 9, match well with the experimental values for the lower molecular weight amines, suggesting that some defects occur even with the smaller amines. There is still a large departure above B620, indicating that large amounts of D2000 can introduce many defects into the networks.

The resins, in other studies, that were well predicted by eqs. (7) or (8) were very different, structurally, compared to the resins used here. This shows that flexible amines can dominate the network properties when paired with shorter more rigid epoxies, although more defects occurred when the length of the flexible amine increased.

Fracture Toughness

Fracture toughness results are shown in Figure 12. D400, B390 (D230), and B440 (D230) had invalid (ductile tearing) results for 40°C. After observing 1–2 samples tear, the remainder of those samples were reconditioned and tested at −20°C.

There is a gradual increase in K_{1c} as the testing temperature approaches the T_gs of the resins. The noticeable increases occur with the B270 (D230) tested at 40°C and the D400 tested at 23°C. The B270 (D230) appears to deviate from the trend but it was one of only two sets that were tested at elevated temperatures. Increased temperature decreases yield stress resulting in higher fracture toughness.[17] Some samples of both the D230 and B270 (D230) tested at 40°C showed visible signs of plastic deformation. Those samples that showed obvious plastic

deformation were not included in the analysis. Other samples, including the room temperature D400 and B440 (D230) samples, showed no visible deformation, despite being tested closer to their respective T_gs, suggesting that above ambient temperatures eases plasticization in these resins, regardless of T_g.

Few samples showed the ideal behavior of a linear load increase followed but an instantaneous drop as fracture occurred. Instead the behavior varied from brittle-stable crack growth, where the load increased linearly until fracture initiated in a slow, controlled manner with no evidence of ductility, to unstable crack growth where the load increased linearly until fracture initiated but then arrested one or more times, resulting in "slip-stick" crack growth. Some samples showed unstable crack growth with no arrest. The cracks were characterized as either stable (S), stable-unstable (S–U) which showed both a crack arrest as well as slow propagation, unstable stick-slip (U-SS) which showed at least one arrest point, or unstable (U) characterized by sharp load decrease with no crack arrest. Similar transitions between types of crack growth with increasing temperature have been seen in other epoxy systems including amine-cured, anhydride-cure,[41] and homopolymerized epoxies; this behavior was seen in both neat and rubber toughened homopolymerized epoxy.[42]

If the fracture data is characterized by the type of fracture, also shown in Figure 12, then the data follow the same trend as seen by Kinloch with the data showing a transition between fracture types as the testing temperature approaches T_g.[42] In the broader transition samples, B390 (D230) and B440 (D230), this transition is shifted to closer to T_g as the samples still show stick-slip behavior whereas the other samples showed unstable behavior. The fracture results are summarized in Table V. Also included in the table are the G_{1c} results calculated either from the area of the load-displacement curve or from K_{1c}. The G_{1c} values are
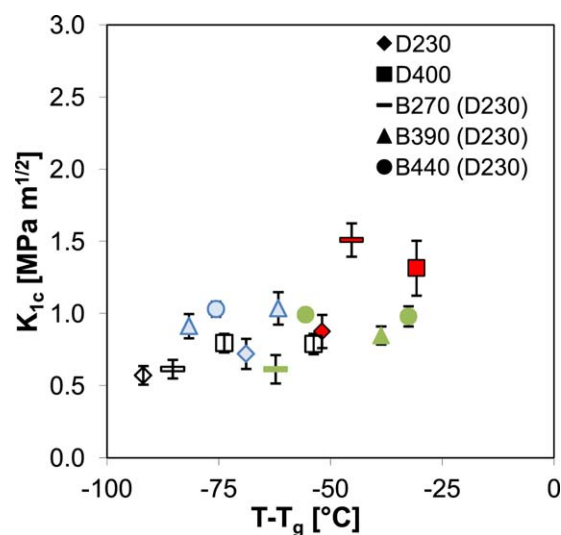

Figure 12. Fracture toughness data plotted vs. $T - T_g$. Symbols signify the formulations as indicated by the legend. Fracture type is indicated by color/fill: Open/no fill: brittle-stable fracture; Light Blue: stable-unstable; Green: unstable-stick slip; Red: unstable. [Color figure can be viewed in the online issue, which is available at wileyonlinelibrary.com.]

Table V. Fracture Properties and Type of Fracture

Resin	Testing T (°C)	$T - T_g$ (°C)	K_{1c} (MPa m$^{1/2}$)	G_{1c} (J/m^2) (from area)	G_{1c} (J/m^2) (from K_{1c})	Facture behavior
D230	0	−92	0.57 ± 0.06	120 ± 70	110 ± 20	S
	23	−69	0.72 ± 0.10	240 ± 150	180 ± 60	S–U–SS
	40	−52	0.88 ± 0.11	370 ± 220	280 ± 80	U
D400	−20	−74	0.80 ± 0.06	280 ± 80	200 ± 30	S
	0	−54	0.79 ± 0.07	190 ± 100	200 ± 40	S
	23	−31	1.31 ± 0.19	670 ± 230	590 ± 180	U
B270 (D230)	0	−85	0.61 ± 0.06	90 ± 40	120 ± 20	S
		−62	0.61 ± 0.10	140 ± 60	130 ± 40	U-SS
	40	−45	1.51 ± 0.12	820 ± 200	840 ± 130	U
B390 (D230)	−20	−82	0.91 ± 0.08	370 ± 140	230 ± 40	S-U
	0	−62	1.04 ± 0.11	380 ± 170	370 ± 80	S-U
	23	−39	0.85 ± 0.06	250 ± 80	280 ± 40	U-SS
B440 (D230)	−20	−76	1.03 ± 0.05	440 ± 110	310 ± 30	S-U
	0	−56	0.99 ± 0.03	560 ± 180	360 ± 30	U-SS
	23	−33	0.98 ± 0.07	510 ± 130	450 ± 60	U-SS

S, Brittle-stable; U-SS, unstable stick-slip; U, unstable.

similar regardless of the calculation method and follow the same trend as K_{1c}.

CONCLUSIONS

Resins were formed by reacting DGEBA with either monodisperse or bimodal blends of polyether amines. The bimodal blends matched the T_g and cross-link density of the resins formed using a single, equivalent molecular weight amine. In the rubbery regions, the density of the blends decreased with increasing amine molecular weight. In the glassy regions, blends containing any amount of D230 approached a similar value, while those containing only D400 or D2000 had consistently lower densities. The glassy modulus of the bimodal amine blends can be greater than those of similar single amine resins, with the modulus increasing with increasing amounts of D2000 for a set temperature below T_g. The T_g was inversely proportional to the volume fraction of amine in the system, while the total damping of the resins was found to be directly proportional. The breath of T_g was dependent on both the volume fraction of amine as well as the amine size, and hence network heterogeneity. The resins with bimodal amines showed greater breath of glass transition and in some cases surpassed the breadth of either amine individually.

The measured M_c values of the epoxy-polyetheramine networks show greater deviation from the theory of rubber elasticity than literature values using either aromatic or short linear amines due to the flexibility of the amines and network defects. The deviations increased with increased average amine molecular weight and can be attributed to cyclization of the D2000. The bimodal blends had little influence on the fracture toughness when plotted versus $T - T_g$, though the broader T_g resins shifted the transition from stable to unstable closer to T_g.

REFERENCES

1. Yee, A. F.; Pearson, R. A. *J. Mater. Sci.* **1986**, *21*, 2462.

2. Yee, A. F.; Pearson, R. A. *J. Mater. Sci.* **1991**, *26*, 3828.

3. Nakamura, Y.; Yamaguchi, M.; Okubo, M.; Matsumoto, T. *J. Appl. Polym. Sci.* **1992**, *45*, 1281.

4. Kinloch, A. J.; Lee, J. H.; Taylor, A. C.; Sprenger, S.; Eger, C. *J. Adhes.* **2003**, *79*, 867.

5. Geisler, B.; Kelley, F. N. *J. Appl. Polym. Sci.* **1994**, *54*, 177.

6. Kim, D. J.; Kang, P. H.; Nho, Y. C. *J. Appl. Polym. Sci.* **2004**, *91*, 1898.

7. Lee, J.; Yee, A. F. *Polymer* **2000**, *41*, 8375.

8. Lee, S. S.; Kim, S. C. *J. Appl. Polym. Sci.* **1997**, *64*, 941.

9. Selby, K.; Miller, L. E. *J. Mater. Sci.* **1975**, *10*, 12.

10. Morgan, R. J.; O'Neal, J. E.; Miller, D. B. *J. Mater. Sci.* **1979**, *14*, 109.

11. Crawford, E.; Lesser, A. J. *J. Polym. Sci. Part B: Polym. Phys.* **1998**, *36*, 1371.

12. Crawford, E. D.; Lesser, A. J. *Polym. Eng. Sci.* **1999**, *39*, 385.

13. Mukherji, D.; Abrams, C. F. *Phys. Rev. E* **2008**, *78*, 050801(R).

14. Mukherji, D.; Abrams, C. F. *Phys. Rev. E* **2009**, *79*, 061802.

15. La Scala, J. J.; Orlicki, J. A.; Winston, C.; Robinette, E. J.; S, J. M.; Palmese, G. R. *Polymer* **2005**, *46*, 2908.

16. Zubeldia, A.; Larranaga, M.; Remiro, P.; Mondragon, I. *J. Polym. Sci. Part B: Polym. Phys.* **2004**, *42*, 3920.

17. Vakil, U. M.; Martin, G. C. *J. Mater. Sci.* **1993**, *28*, 4442.

18. St. John, N. A.; George, G. A. *Polymer* **1992**, *33*, 2679.

19. Menard, K. Dynamic Mechanical Analysis: A Practical Introduction, 2nd ed; CRC Press: Boca Raton, **2008**.

20. Nielsen, L. E.; Landel, R. F. Mechanical Properties of Polymers and Composites, 2nd ed. Marcel Dekker Inc.: New York, **1994**.

21. Flory, P. J. Principles of Polymer Chemistry; Cornell University Press: Ithaca, **1953**.

22. Nakka, J. S.; Jansen, K. M. B.; Ernst, L. J.; Jager, W. F. *J. Appl. Polym. Sci.* **2008**, *108*, 1414.

23. Ma, J.; Qi, Q.; Bayley, J.; Du, X.-S.; Mo, M.-S.; Zhang, L. Q. *Polym. Test.* **2007**, *26*, 445.

24. Marks, M. J.; Snelgrove, R. V. *Appl. Mater. Interfaces*, **2009**, *1*, 92124.

25. Lesser, A. J.; Crawford, E. *J. Appl. Polym. Sci.*, **1997**, *66*, 387.

26. Cuddihy, E.; Moacanin, J. In Epoxy Resins; Gould, R. F., Ed.; Advances in Chemistry Series 92; American Chemical Society: Washington, DC, **1970**; pp 96–107.

27. Williams, J. G. *J. Appl. Polym. Sci.* **1979**, *23*, 3433-3444.

28. Shi, J. F.; Inglefield, P. T.; Jones, A. A.; Meadows, M. D. *Macromolecules* **1996**, *29*, 605.

29. McGrath, L. M.; Parnas, R. S.; King, S. H.; Schroeder, J. L.; Fischer, D. A.; Lenhart, J. L. *Polymer* **2008**, *48*, 999.

30. Kwak, G.-H.; Park, S.-L.; Lee, J.-R. *J. Appl. Polym. Sci.* **2000**, *78*, 290.

31. He, Y.; Zhu, B.; Inoue, Y. *Prog. Polym. Sci.* **2004**, *29*, 1021.

32. Fox, T. G. *Bull. Am. Phys. Soc.* **1956**, *1*, 123.

33. Chang, M. C. O.; Thomas, D. A.; Sperling, L. H. *J. Appl. Polym. Sci.* **1987**, *34*, 409.

34. Scanlan, J. *J. Polym. Sci.* **1960**, *43*, 501.

35. Hill, L. W. *Prog. Org. Coat.* **1997**, *31*, 235.

36. Charlesworth, J. M. *Polym. Eng. Sci.* **1988**, *28*, 230.

37. Miller, D. R.; Macosko, C. W. *Macromolecules* **1976**, *9*, 206.

38. LeMay, J. D.; Kelley, F. N. *Adv. Polym. Sci.* **1986**, *78*, 115.

39. Graessley, W. *Macromolecules* **1975**, *8*, 186.

40. Flory, P. J. *Polymer* **1979**, *20*, 1317.

41. Zhang, Z.; Evans, D. *Polym. Eng. Sci.* **2003**, *43*, 1071.

42. Kinloch, A. J.; Shaw, S. J.; Tod, D. A.; Hunston, D. L. *Polymer* **1983**, *24*, 1341.